PROCEEDINGS OF SCIENCE

Semileptonic $B \to \pi\ell\nu$, $B \to D\ell\nu$, $B_s \to K\ell\nu$, and $B_s \to D_s\ell\nu$ decays

Jonathan Flynn

Physics and Astronomy, University of Southampton, Southampton SO17 1BJ, UK

Ryan Hill*

Physics and Astronomy, University of Southampton, Southampton SO17 1BJ, UK
DISCnet Centre for Doctoral Training, University of Southampton, Southampton SO17 1BJ, UK
E-mail: R.C.Hill@soton.ac.uk

Andreas Jüttner

Physics and Astronomy, University of Southampton, Southampton SO17 1BJ, UK
STAG Research Center and Mathematical Sciences, University of Southampton, Southampton SO17 1BJ, UK

Amarjit Soni

Physics Department, Brookhaven National Laboratory, Upton, NY 11973, USA

Justus Tobias Tsang

Higgs Centre for Theoretical Physics, The University of Edinburgh, EH9 3FD, UK
CP3-Origins and IMADA, University of Southern Denmark, Campusvej 55, 5230 Odense M, Denmark

Oliver Witzel*

Department of Physics, University of Colorado Boulder, Boulder, CO 80303, USA
E-mail: Oliver.Witzel@colorado.edu

We present updates for our nonperturbative lattice QCD calculations to determine semileptonic form factors for exclusive $B \to \pi\ell\nu$, $B \to D\ell\nu$, $B_s \to K\ell\nu$, and $B_s \to D_s\ell\nu$ decays. Our calculation is based on RBC-UKQCD's set of $2+1$-dynamical-flavor gauge field ensembles. In the valence sector we use domain wall fermions for up/down, strange and charm quarks, whereas bottom quarks are simulated with the relativistic heavy quark action. The continuum limit is based on three lattice spacings. Using kinematical z expansions we aim to obtain form factors over the full q^2 range. These form factors are the basis for predicting ratios addressing lepton flavor universality or, when combined with experimental results, to obtain CKM matrix elements $|V_{ub}|$ and $|V_{cb}|$.

The 37th Annual International Symposium on Lattice Field Theory – LATTICE2019
16–22 June 2019
Wuhan, China

*Speaker.
†Combined contribution of both speakers.

PoS(LATTICE2019)184

1. Introduction

The Standard Model (SM) of elementary particle physics has been tested in numerous processes over recent decades and the overall agreement between theoretical predictions and experimental observations is astonishing. The SM successfully describes three of the four fundamental forces in nature: electromagnetic, weak, and strong, with only gravitation not included. Although successful, the SM is an effective theory and corrections due to 'new physics' are expected to occur at higher energies. In order to observe such effects, one possibility is to perform precision tests of SM-allowed processes, which requires both experimental and theoretical effort [1]. Particularly interesting are weak quark-flavor-changing transitions.

Quark flavor mixing is typically described by the Cabibbo-Kobayashi-Maskawa (CKM) matrix which is a unitary 3×3 matrix in the SM. Testing the unitarity of the CKM matrix remains a major focus of the experimental and theoretical research program. Decays involving bottom (or b) quarks are most promising because, compared to the light sector, theoretical predictions are currently less precise and the much larger mass of the b quark allows many decay channels. Experimentally, interactions of b quarks can be studied by looking for B-mesons and their decays. Two current experiments, Belle II [2] and LHCb [3], are dedicated to B-physics but ATLAS and CMS also study such processes. At present the b sector of the SM exhibits various tantalizing tensions between experimental measurements and theoretical predictions. Most noteworthy are the signs of lepton flavor universality violation observed in semileptonic decays. $B \to D^{(*)}\ell\nu$ decays probe the transition of a b quark to a c quark, and forming the ratio of processes with a heavy $\tau\nu_\tau$ lepton pair in the final state to those containing the much lighter $\mu\nu_\mu$ (or $e\nu_e$), defines the R-ratio

$$R^{\tau/\mu}_{D^{(*)}} \equiv \frac{BF(B \to D^{(*)}\tau\nu_\tau)}{BF(B \to D^{(*)}\mu\nu_\mu)}. \tag{1.1}$$

Experimentally this ratio has been determined by BaBar, Belle and LHCb [4 – 13] and the SM predictions are based on [14 – 17]. The average experimental and theoretical values exhibit at present a discrepancy of about 3σ [18]. Since many uncertainties cancel, this ratio is a theoretically clean quantity and hence a strong test of the SM. Furthermore, these semileptonic decays allow extraction of the CKM matrix element $|V_{cb}|$ by combining experimental and theoretical results. The determination based on these exclusive channels exhibits a 2–3σ tension with that from inclusive $B \to X_c\ell\nu$ where X_c denotes any final state containing a charm quark [19 – 21, 1]. A similar tension is observed for the CKM matrix element $|V_{ub}|$ where the exclusive $B \to \pi\ell\nu$ and the inclusive $B \to X_u\ell\nu$ channels are typically considered, with X_u being a charmless final state containing an up-quark.

These investigations are based on branching fractions (BF) which are experimentally measured and conventionally parameterized by

$$\frac{d\Gamma(B_{(s)} \to P\ell\nu)}{dq^2} = \frac{\eta_{EW} G_F^2 |V_{xb}|^2}{24\pi^3} \frac{(q^2 - m_\ell^2)^2 \sqrt{E_P^2 - M_P^2}}{q^4 M_{B_{(s)}}^2} \times \left[\left(1 + \frac{m_\ell^2}{2q^2}\right) M_{B_{(s)}}^2 (E_P^2 - M_P^2) |f_+(q^2)|^2 + \frac{3m_\ell^2}{8q^2} (M_{B_{(s)}}^2 - M_P^2)^2 |f_0(q^2)|^2 \right]. \tag{1.2}$$

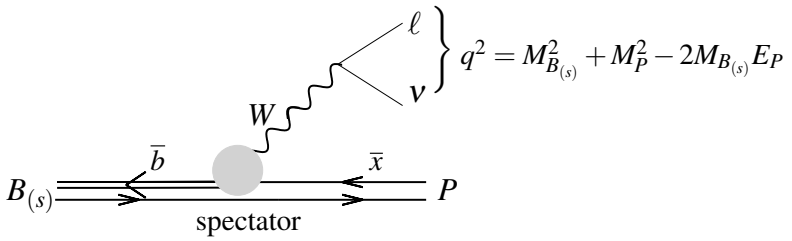

Figure 1: Sketch of tree-level weak semileptonic $B_{(s)}$ decays mediated by a charged $W^\pm$ boson in a set-up with the $B_{(s)}$ meson at rest. P denotes a pseudoscalar final state (π, K, D, or D_s), the spectator is a light up/down or a strange quark, and x the up or charm daughter quark.

In Eq. (1.2) we focus solely on semileptonic $B_{(s)}$ decays mediated by a charged current with a pseudoscalar particle (P) in the final state as sketched in Fig. 1. M_P is the mass of this particle, E_P its energy, and $|V_{xb}|$ is the CKM matrix of interest with $x = u, c$. The four-momentum transferred to the leptonic products of type $\ell = e, \mu, \tau$ is denoted by q^μ and m_ℓ is the mass of the lepton. On the theoretical side, the determination faces the challenge that nonperturbative interactions due to the strong force contribute, parametrized by the form factors f_+ and f_0, whereas G_F is the perturbatively-computed Fermi constant. Lattice quantum chromodynamics (QCD) provides a state-of-the-art nonperturbative framework for determining the form factors. An overview of existing results based on lattice QCD as well as averages obtained from them can be found in [22]. Here we focus on four semileptonic $B_{(s)}$ decay channels which have been calculated by

$B \to \pi\ell\nu$:	HPQCD [23], Fermilab/MILC [24, 25], RBC/UKQCD[26]
$B \to D\ell\nu$:	Fermilab/MILC [27, 28], HPQCD [29]
$B_s \to K\ell\nu$:	HPQCD [30], RBC/UKQCD[26], Alpha [31], Fermilab/MILC [32]
$B_s \to D_s\ell\nu$:	Fermilab/MILC [33, 32], HPQCD [34, 35]

In addition several groups report on work in progress [36 – 40]; see also work referred in [41].

As indicated in Fig. 1, all four processes change the flavor of the b quark in the initial state by emission of a charged $W^\pm$ boson. The spectator quark is an up or down quark for B decays and a strange quark for B_s decays. The daughter quark is either an up or charm quark to allow π, D or K, D_s final states, respectively.

We present these four channels together because in our set-up only the bottom quark is simulated by the relativistic heavy quark (RHQ) action [42, 43] whereas up/down, strange, and charm quarks are simulated using domain wall fermions (DWF) [44 – 49]. We use the RBC-UKQCD $2+1$-flavor domain wall fermion and Iwasaki gauge action ensembles [50 – 53], and list their key properties in Tab. 1. The F1 ensemble is a new addition compared to our previous publications [54, 26, 55]. It provides a third, finer lattice spacing as well as a data point closer to the physical pion mass. This further constrains the extrapolations to the continuum limit and to the physical light quark mass. In the valence sector we use the unitary light quark mass for u/d quarks and choose a close-to-physical value for the strange quark mass. Charm quarks are simulated using a domain wall action optimized for heavy flavors [56, 57]. For the coarse ensembles (C1, C2), three 'lighter-than-charm' masses are simulated and we subsequently perform a benign extrapolation, whereas for the medium fine (M1, M2, M3) and fine (F1) ensembles we bracket the physical charm quark mass and interpolate. As mentioned above, bottom quarks are simulated with

	$L^3 \times T$	a^{-1} / GeV	am_l	M_π / MeV	# Configurations	# Time Sources
C1	$24^3 \times 64$	1.784	0.005	338	1636	1
C2	$24^3 \times 64$	1.784	0.010	434	1419	1
M1	$32^3 \times 64$	2.383	0.004	301	628	2
M2	$32^3 \times 64$	2.383	0.006	362	889	2
M3	$32^3 \times 64$	2.383	0.008	411	544	2
F1	$48^3 \times 96$	2.774	0.002144	234	98	24

Table 1: The RBC-UKQCD 2+1 domain-wall fermion ensembles used in this work [50–53]. The F1 ensemble is a new element of the RBC/UKQCD b-physics project analysis and is a key difference between this work and the prior analysis. Presently the properties of the F1 ensemble are re-evaluated and may change slightly.

the effective RHQ action, with nonperturbatively tuned parameters [58] which have been updated compared to our previous work to reflect improved determinations of the lattice spacing.

The form factors introduced in Eq. (1.2) can be determined by computing the hadronic matrix elements $\langle P|\mathscr{V}^\mu|B_{(s)}\rangle$, parameterized as

$$\langle P(p_P)|\mathscr{V}^\mu|B_{(s)}(p_{B_{(s)}})\rangle = f_+(q^2)\left(p^\mu_{B_{(s)}} + p^\mu_P - \frac{M^2_{B_{(s)}} - M^2_P}{q^2}q^\mu\right) + f_0(q^2)\frac{M^2_{B_{(s)}} - M^2_P}{q^2}q^\mu\,, \quad (1.3)$$

with $p_{B_{(s)}}$ and p_P the momenta of the $B_{(s)}$ and P mesons respectively, and $\mathscr{V}^\mu = \bar{x}\gamma^\mu b$. In our calculation we place the initial $B_{(s)}$ meson at rest and use an alternative parameterization of the matrix elements in terms of the perpendicular and parallel components

$$\langle P|\mathscr{V}^\mu|B_{(s)}\rangle = \sqrt{2M_{B_{(s)}}}\left[v^\mu f_\parallel(E_P) + p^\mu_\perp f_\perp(E_P)\right]\,, \quad (1.4)$$

with $p^\mu_\perp \equiv p^\mu_P - (p_P\cdot v)v^\mu$. Hence we determine the form factors

$$f_\parallel = \frac{\langle P|\mathscr{V}^0|B_{(s)}\rangle}{\sqrt{2M_{B_{(s)}}}}, \qquad f_\perp = \frac{\langle \pi|\mathscr{V}^i|B_{(s)}\rangle}{\sqrt{2M_{B_{(s)}}}}\frac{1}{p^i_P} \quad (1.5)$$

and obtain the phenomenological form factors f_+ and f_0 from

$$f_+(q^2) = \frac{1}{\sqrt{2M_{B_{(s)}}}}\left[f_\parallel(q^2) + (M_{B_{(s)}} - E_P)f_\perp(q^2)\right], \quad (1.6)$$

$$f_0(q^2) = \frac{\sqrt{2M_{B_{(s)}}}}{M^2_{B_{(s)}} - M^2_P}\left[(M_{B_{(s)}} - E_P)f_\parallel(q^2) + (E^2_P - M^2_P)f_\perp(q^2)\right]. \quad (1.7)$$

For the lattice determination we evaluate Eq. (1.5) by computing three-point and two-point correlation functions on the lattice. The operators entering the three-point functions include tree-level plus 1-loop $O(a)$-improved terms with perturbatively calculated improvement coefficients. The hadronic matrix elements are obtained by performing correlated fits to ratios of these three-point and two-point functions using the bootstrap resampling technique. In order to test for systematic

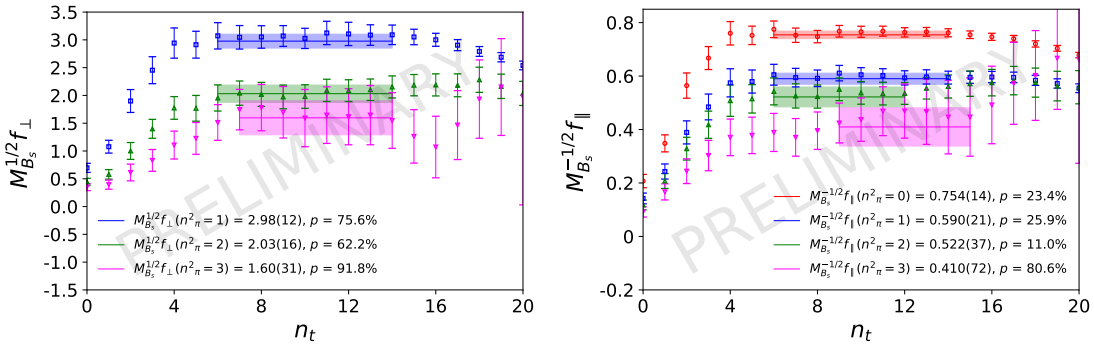

Figure 2: Plateau fits to ratios of three-point and two-point functions used to determine $f_\perp$ and $f_\parallel$ on the M1 ensemble for $B \to \pi\ell\nu$ semileptonic decays.

effects due to excited state contributions, we fit to a simple plateau assuming only ground state contributions, but also with additional terms to describe one added excited state for the initial as well as the final state. The matrix elements containing the vector current $\mathcal{V}_\mu$ are finally renormalized to obtain continuum expressions

$$\langle P|\mathcal{V}_\mu|B_{(s)}\rangle = Z_\mu^{bx}\langle P|V_\mu|B_{(s)}\rangle\,. \tag{1.8}$$

The heavy-light renormalization factor Z_μ^{bx} is obtained using a 'mostly nonperturbative' ansatz [59]

$$Z_{V_\mu}^{bx} = \rho_{V_\mu}^{bx}\sqrt{Z_\mu^{bb}Z_\mu^{xx}}, \tag{1.9}$$

where the flavor conserving factors Z_μ^{bb} and Z_μ^{xx} are computed nonperturbatively and the remaining factor $\rho_{V_\mu}^{bx}$ is determined at 1-loop in lattice perturbation theory.

In the following Section we will report on the status of the four decay channels. We start with our more preliminary determinations of form factors for $B \to \pi\ell\nu$ and $B \to D\ell\nu$ and continue with the more advanced results for $B_s \to K\ell\nu$ and $B_s \to D_s\ell\nu$. In Section 3 we present details of the kinematical z-expansion followed by a brief summary. The determinations of $B \to \pi\ell\nu$ and $B_s \to K\ell\nu$ form factors update our results from 2015 [26].

2. Semileptonic form factors

2.1 $B \to \pi\ell\nu$

Following the steps outlined above, we first determine $f_\parallel$ and $f_\perp$ on all six of our ensembles. Figure 2 shows an example of fits to extract the plateau values. Having determined and renormalized the form factors from the lattice data, we obtain the chiral-continuum limit by performing correlated global fits to all data points. The fit function is derived from SU(2) heavy meson chiral perturbation theory in the hard-pion limit [60, 61]

$$f^{B\to\pi}(M_\pi, E_\pi, a) = \frac{1}{E_\pi + \Delta}c_0\left[1 + \frac{\delta f^{B\to\pi}}{(4\pi f_\pi)^2} + c_1\frac{M_\pi^2}{\Lambda^2} + c_2\frac{E_\pi}{\Lambda} + c_3\frac{E_\pi^2}{\Lambda^2} + c_4(a\Lambda)^2\right]. \tag{2.1}$$

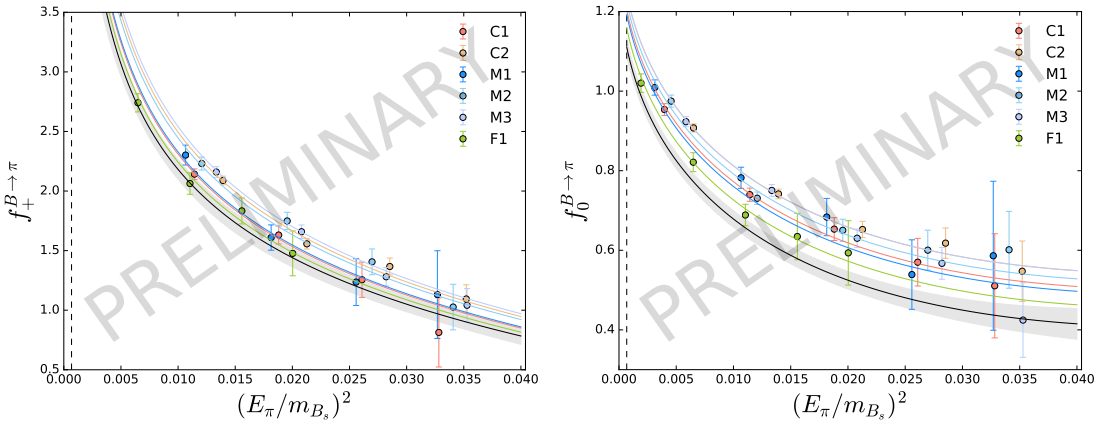

Figure 3: $B \to \pi\ell\nu$ chiral-continuum fit to the f_+ and f_0 data using heavy meson chiral perturbation theory. The determination of the form factors at discretized momenta for our six ensembles are shown by the colored symbols and the chiral-continuum limit is denoted by the black line with gray error band. Only statistical errors are shown in the plots.

In the equation above, $\Delta = M_{B^*} - M_B$ and B^* is a $\bar{b}u$ flavor state with quantum numbers $J^P = 1^-$ for f_+, or $J^P = 0^+$ for f_0. Since for $B \to \pi\ell\nu$ decays only the vector B^* meson lies below the production threshold, we include the pole factor $1/(E_\pi + \Delta)$ only for f_+ but not for f_0. The non-analytic term is

$$\delta f^{B\to\pi} = -\frac{3}{4}(3g_b^2 + 1)M_\pi^2 \log\left(\frac{M_\pi^2}{\Lambda^2}\right), \tag{2.2}$$

where f_π is the pion decay constant, Λ a reference scale of $O(1\,\text{GeV})$, and g_b is the $B^*B\pi$ coupling constant determined in Ref. [55]. The final chiral-continuum limit for f_+ and f_0 is shown by the black line with gray error band in the plots in Fig. 3 whereas the colored data points are our renormalized lattice data and the colored lines show the fit results at finite lattice spacing and unphysical *u*/*d* quark masses. The plots in Fig. 3 cover the energy range we can directly simulate on our set of ensembles. Exploring more energetic pions is challenging because the signal-to-noise ratio deteriorates as the pion momentum increases.

We therefore construct a set of synthetic data points from the continuum description of the form factors and estimate all systematic uncertainties for these points. A complete error budget can then be fed into a kinematical z-expansion to obtain form factors covering the full range of physically allowed momentum transfer q^2. Details of the z-expansion are described in Sec. 3.

2.2 $B \to D\ell\nu$

The determination of $B \to D\ell\nu$ form factors requires us to simulate charm quarks. We do so using DWF optimized for heavy quarks [57]. On the coarse ensembles this formulation does not allow us to reach physical charm quark masses and we therefore simulate three values lighter than the charm quark mass. On the medium fine and fine ensembles, however, we do reach the physical charm quark mass and bracket its value. In Fig. 4 we show the renormalized form factors f_+ and f_0 for five of our six ensembles and the set of three or two charm quark masses.

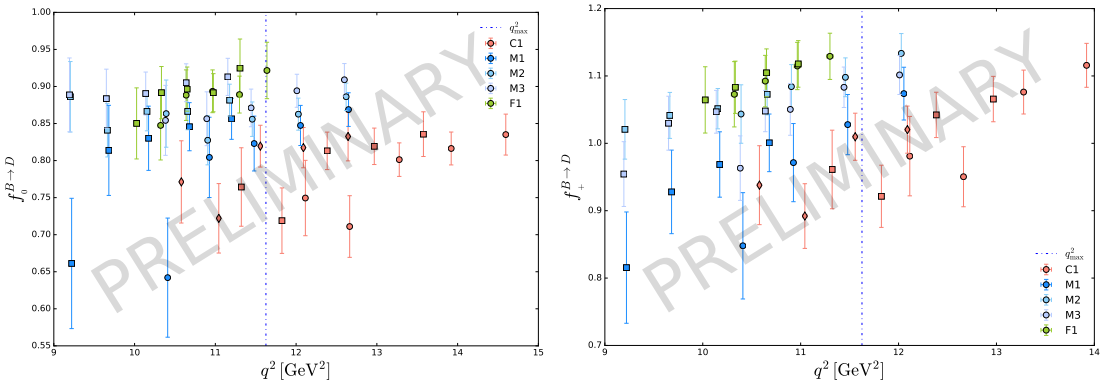

Figure 4: Form factors f_+ and f_0 for $B \to D\ell\nu$ semileptonic decays. Since we either extrapolate three 'lighter-than-charm' quark masses or interpolate bracketing charm quark masses, several sets of data points are shown for each ensemble.

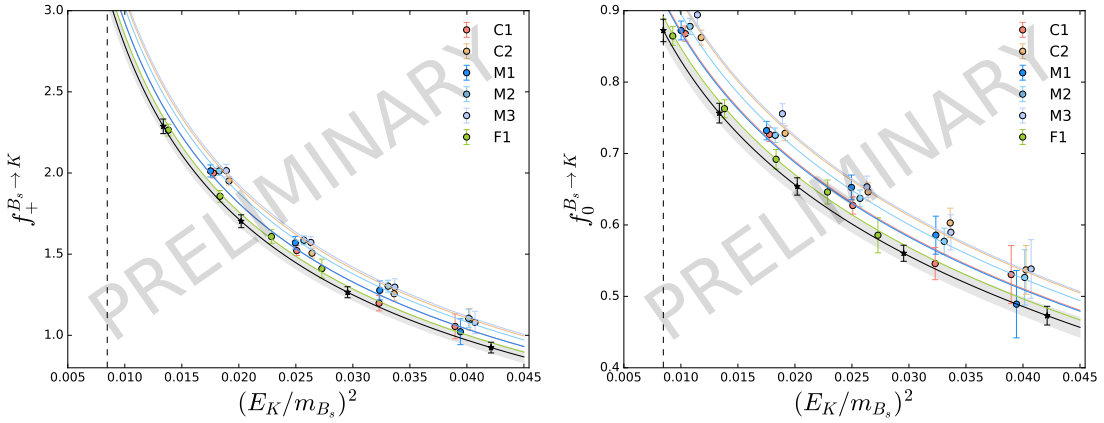

Figure 5: Chiral-continuum extrapolation for $B_s \to K\ell\nu$ decays using SU(2) hard-kaon heavy meson χPT. Colored symbols show the form factors determined on our six ensembles and the black line with gray error band the result of the chiral-continuum extrapolation. Only statistical uncertainties are shown.

As for $B \to \pi\ell\nu$ the next step is to perform a chiral-continuum extrapolation to the continuum and to physical light quark masses by performing a fit to all data points. In addition, we need to include an extra(inter)polation to the physical charm quark mass. We are currently investigating different fit ansätze and also compare a global fit performing all extrapolations at once compared to a two step fit separating the charm extra(inter)polation from the chiral-continuum extrapolation.

2.3 $B_s \to K\ell\nu$

The $B_s \to K\ell\nu$ analysis follows the $B \to \pi\ell\nu$ analysis presented in Subsection 2.1. Since only one light u quark enters in the valence sector, the chiral extrapolation is milder and the data is statistically more precise as can be seen in Fig. 5. As above, the colored symbols refer to the form factors determined on our six ensembles and the colored lines show the outcome of the chiral-continuum extrapolation at finite lattice spacing and unphysical light quark masses whereas the black line with gray error band shows the result in the chiral-continuum limit. For this process we

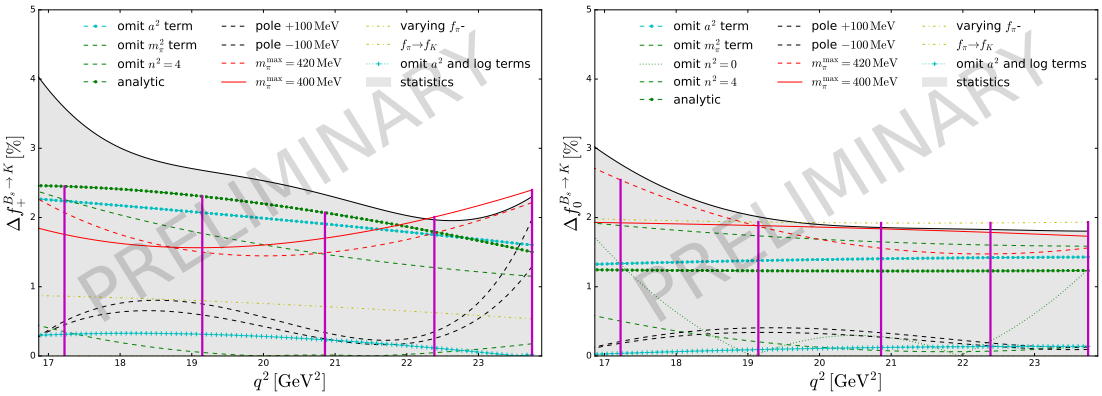

Figure 6: Preliminary estimate of systematic uncertainties for the determination of $B_s \to K\ell\nu$ form factors due to variations of the fit ansatz which is based on SU(2) heavy meson chiral perturbation theory. Vertical magenta lines indicate the q^2 values used in the subsequent z expansion.

again use a fit ansatz based on SU(2) heavy meson chiral perturbation theory and consider the hard kaon limit. The fit function is obtained from Eq. (2.1) by substituting π with K and using

$$\delta_f^{B_s \to K} = -\frac{3}{4} M_\pi^2 \log\left(\frac{M_\pi^2}{\Lambda^2}\right). \tag{2.3}$$

Further a pole factor is present for both form factors, $f_\perp$ and $f_\parallel$, in the case of $B_s \to K\ell\nu$ extrapolations. Fig. 5 shows in addition, with black crosses, the synthetic data points we will use subsequently to perform the kinematical extrapolation over the full range of momentum transfer. As a first step to estimate systematic uncertainties, we perform variations of our fit ansatz. In Fig. 6 we show relative deviations over our preferred fit as a function of the q^2 range covered by our data. The gray error band indicates the statistical uncertainty of our preferred fit and the colored lines indicate different variations. Variations of our fit ansatz include adding higher order or removing terms from the fit function, applying different cuts to our data, or varying external parameters entering the fit function. As is shown in the figure, most of these variations change the central value by less than our statistical uncertainty. In addition we need to estimate systematic effects originating, for example, from the lattice spacing, RHQ parameters, strange quark mass, or renormalization coefficients. Some of these uncertainties are already in place, work is in progress to estimate others. Here we use a preliminary estimate to obtain synthetic data points with a combined statistical and systematic uncertainty. These data points are the input for the z-expansion presented in Sec. 3.1.

2.4 $B_s \to D_s\ell\nu$

For the $B_s \to D_s\ell\nu$ form factors, we simulate a set of charm quark masses and then extra(inter)polate to the physical value, as described in Subsection 2.2. Hence in Fig. 7 we again show a set of data points for each of our six ensembles. Since the $B_s \to D_s\ell\nu$ decays do not have light quarks in the valence sector, we perform a global fit based on a Padé approximation in order

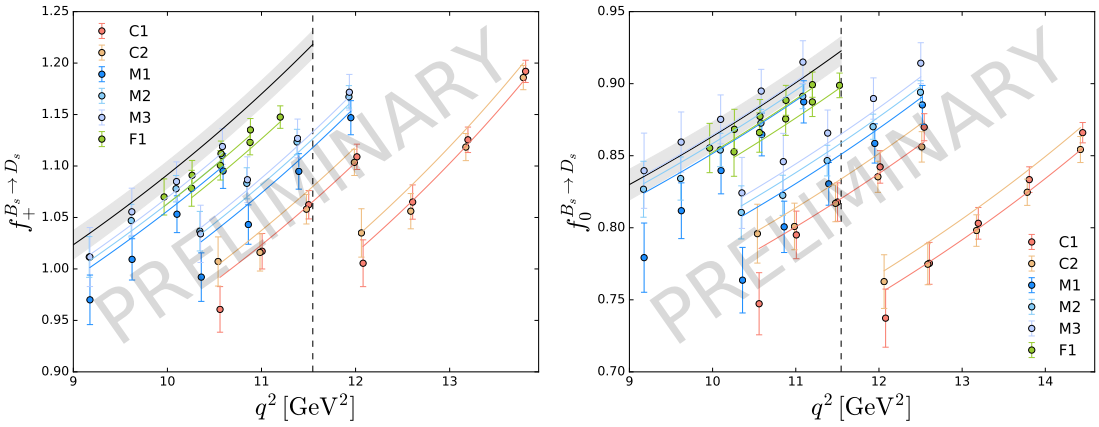

Figure 7: Global fit extrapolating our $B_s \to D_s\ell\nu$ form factors to physical quark masses and the continuum limit (gray band). The colored lines show the fit result at the different unphysical charm quark masses.

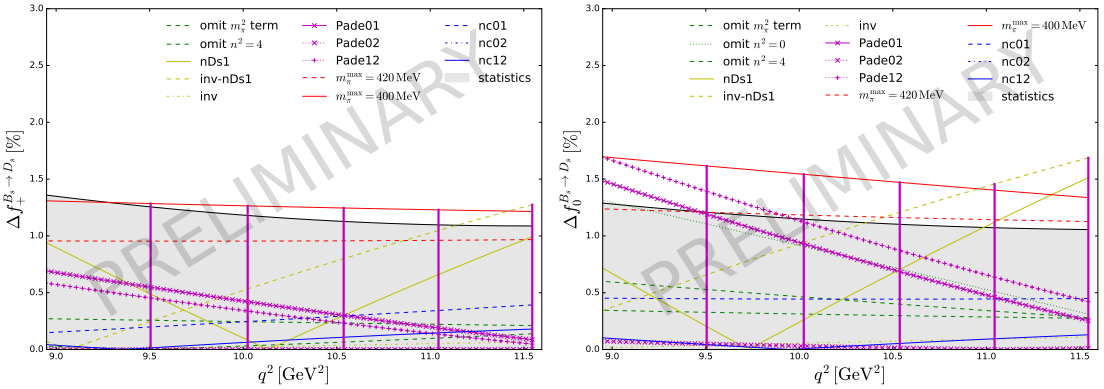

Figure 8: Preliminary estimate of systematic uncertainties for the determination of $B_s \to D_s\ell\nu$ form factors due to variations of the fit ansatz. Vertical magenta lines indicate the q^2 values used in the subsequent z expansion.

to extrapolate to physical quark masses and the continuum limit

$$f(q^2,a,M_\pi,M_{D_s}) = \left[c_0 + c_1\frac{M_\pi^2}{\Lambda^2} + \sum_{j=1}^{n_{D_s}} c_{2,j}\left[\Lambda\cdot\Delta M_{D_s}^{-1}\right]^j + c_3(a\Lambda)^2\right] P_{\alpha,\beta}(q^2/M_{B_s}^2), \tag{2.4}$$

$$\text{with}\quad \Delta M_{D_s}^{-1} \equiv \left(\frac{1}{M_{D_s}} - \frac{1}{M_{D_s}^{\text{phys}}}\right) \quad\text{and}\quad P_{\alpha.\beta}(x) = \frac{1+\sum_{i=1}^{N_\alpha}\alpha_i x^i}{1+\sum_{i=1}^{N_\beta}\beta_i x^i}.$$

Λ is again a reference scale of of order 1 GeV. The colored lines in Fig. 7 show the fit result at unphysical charm quark mass and the gray band the form factors at physical quark masses in the continuum. As for the $B_s \to K\ell\nu$ decays described above, we perform variations of our fit ansatz to estimate its systematic uncertainty. Examples are shown in Fig. 8. Estimates of other systematic effects are ongoing and we therefore use a preliminary error budget as input for the z-expansion shown in Subsection 3.2.

3. Kinematical z-expansion

As shown in the previous Section, the lattice calculation of semileptonic form factors for $B_{(s)}$ decays directly covers the region of large momentum transfer (large q^2) and is most precise near $q^2_{\rm max}$. To extend the range to small momentum transfer, we perform an additional, kinematical extrapolation typically referred to as a z-expansion. As input for the z-expansion we use 'synthetic' data points extracted from our results after extrapolation to physical quark masses and to the continuum. For these points we estimate full systematic uncertainties and hence obtain a set of form-factor data points at specific q^2 values with full, statistical and systematic, uncertainties to be used for the kinematical extrapolation. Although the systematic error budget is not yet complete, we outline the next steps of the analysis.

In a first step the complex q^2 plane with a cut for $q^2 \geq t_+$ is mapped onto the unit disk in z with the transformation

$$z(q^2,t_0) = \frac{\sqrt{1-q^2/t_+}-\sqrt{1-t_0/t_+}}{\sqrt{1-q^2/t_+}+\sqrt{1-t_0/t_+}}, \tag{3.1}$$

where $t_- = (M_{B_{(s)}} - M_P)^2$ for $P = \pi, KD, D_s$, and t_+ is fixed by the appropriate two-particle production threshold. In the case of $B \to \pi\ell\nu$ and $B_s \to K\ell\nu$, the start of the cut is given by $t_+ = (M_B + M_\pi)^2$, whereas for $B \to D\ell\nu$ and $B_s \to D_s\ell\nu$ the cut begins at $t_+ = (M_B + M_D)^2$. Using t_+ and t_- we define $t_0 = t_+ - \sqrt{t_+(t_+ - t_-)}$. Commonly two different implementations of the z-expansion are considered for our processes of interest. Boyd, Grinstein, and Lebed (BGL) [62] express the form factors ($X = +, 0$) as

$$f_X(q^2) = \frac{1}{B_X(q^2)\phi_X(q^2,t_0)} \sum_{n=0}^{N} a_n(t_0) z^n, \tag{3.2}$$

where ϕ_X are outer functions and B_X are the Blaschke factors which vanish at the positions of sub-threshold poles (so that the remaining z-dependence can be expanded in a power series). The a_n coefficients are subject to a constraint derived from a dispersive bound

$$\sum_{n=0}^{\infty} a_n^2(t_0) \leq 1. \tag{3.3}$$

An alternative implementation is given by Bourrely, Caprini, and Lellouch (BCL) [63] who, for $X = +$ in $B \to \pi$ semileptonic decay, parametrized the form factor by

$$f_X(q^2) = \frac{1}{1 - q^2/M^2_{\rm pole}} \sum_{k=0}^{K} b_k(t_0) z^k, \tag{3.4}$$

with the constraints

$$\sum_{n=0}^{\infty} a_n^2 = \sum_{j=0}^{K}\sum_{k=0}^{K} b_j B_{jk} b_k \leq 1 \qquad \text{and} \qquad \sum_{k=0}^{K} (-1)^{k-1} k b_k(t_0) = 0. \tag{3.5}$$

The first constraint in Eq. (3.5) is derived by equating the expressions in (3.2) and (3.4) and expanding the known functions in powers of z in order to relate the a_n and b_n and hence determine the B_{jk}. The second constraint applies only to f_+ and originates from angular momentum conservation.

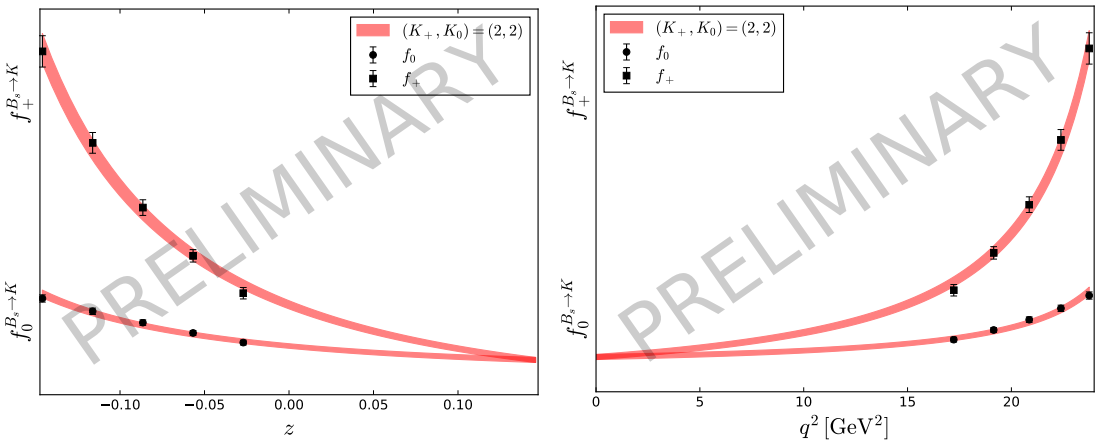

Figure 9: Preliminary kinematical extrapolation (z-expansion) of our $B_s \to K\ell\nu$ form factors over the full q^2 range using the BCL parametrization. The extrapolation is performed using a set of five synthetic data points (black symbols) which are obtained with a non-final error budget.

3.1 $B_s \to K\ell\nu$

Using our results of Section 2.3 with a preliminary error budget for the synthetic data points, we perform a kinematical extrapolation down to $q^2 = 0$. We use the BCL parametrization described above with a pole mass $M_{\rm pole} = M_{B^*} = 5.33\,\text{GeV}$ for f_+, and no pole for f_0, since the theoretically predicted $B^*(0^+)$ mass, 5.63 GeV [64] is above $M_B + M_\pi$. The outcome is shown in Fig. 9. On the left we present the resulting form factors in z-space, on the right we convert back to q^2.

Once our systematic errors have been finalized, we have everything in place to obtain the form factors with full q^2 dependence. Integrating these form factors over q^2, we can derive predictions to test the universality of lepton flavors

$$R_K^{\tau/\mu} \equiv \frac{BF(B_s \to K\tau\nu_\tau)}{BF(B_s \to K\mu\nu_\mu)}. \tag{3.6}$$

or compare our results to the determination by HPQCD [30], Alpha [31], or Fermilab/MILC [32].

3.2 $B_s \to D_s\ell\nu$

In the case of $B_s \to D_s\ell\nu$ decays we proceed similarly. Starting from the synthetic data points with preliminary error budget obtained in Section 2.4, we perform a BCL-style z-expansion using at present pole masses $M_+ = M_{B_c^*} = 6.33$ GeV and $M_0 = 6.69$ GeV [65]. Figure 10 shows again on the left the resulting form factors vs. z and on the right vs. q^2. A finalized error budget will allow us to compare our results to the determination by HPQCD [34, 35] and Fermilab/MILC [33, 32]. In addition we can calculate

$$R_{D_s}^{\tau/\mu} \equiv \frac{BF(B_s \to D_s\tau\nu_\tau)}{BF(B_s \to D_s\mu\nu_\mu)}, \tag{3.7}$$

to test lepton flavor universality.

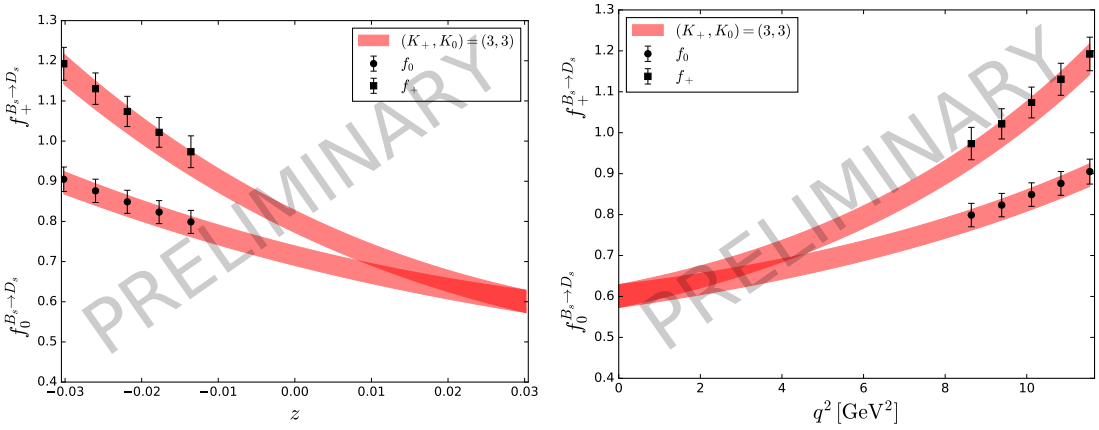

Figure 10: Preliminary kinematical extrapolation (z-expansion) of our $B_s \to D_s\ell\nu$ form factors over the full q^2 range using the BCL parametrization. The extrapolation is performed using a set of five synthetic data points (black symbols) which are obtained with a non-final error budget.

4. Summary

We have reported updates on the RBC-UKQCD B-physics program which currently has the main focus to calculate form factors of semileptonic decays. Our set-up features b-quarks simulated with the RHQ action but uses DWF for up/down, strange, and charm quarks. Here we presented the status of our analysis for $B \to \pi\ell\nu$, $B \to D\ell\nu$, $B_s \to K\ell\nu$, and $B_s \to D_s\ell\nu$. In addition to the charged current decays with pseudoscalar final state, our framework also includes operators to determine $W^{\pm}$ mediated decays to vector final states as well as Glashow-Iliopoulos-Maiani (GIM) suppressed neutral current decays [66, 67].

In parallel we are continuing our efforts to advance the use of heavy DWF for b quarks and extend the methods used in the calculation of decay constants [53] or neutral meson mixing matrix elements [68] to semileptonic decays [69].

Acknowledgments

We thank our RBC and UKQCD collaborators for helpful discussions and suggestions, and P. Gambino for discussion on unitarity-constrained fits. Computations were performed on resources provided by the USQCD Collaboration, funded by the Office of Science of the U.S. Department of Energy, on the ARCHER UK National Supercomputing Service (http://www.archer.ac.uk), as well as on computers at Columbia University and Brookhaven National Laboratory. We used gauge field configurations generated on the DiRAC Blue Gene Q system at the University of Edinburgh, part of the DiRAC Facility, funded by BIS National E-infrastructure grant ST/K000411/1 and STFC grants ST/H008845/1, ST/K005804/1 and ST/K005790/1. This project has received funding from STFC grants ST/L000458/1 and ST/P000711/1. RH was supported by the DISCnet Centre for Doctoral Training (STFC grant ST/P006760/1). AS was supported in part by US DOE contract DE–SC0012704. OW acknowledges support from DOE grant DE–SC0010005. No new experimental data was generated.

References

[1] PARTICLE DATA GROUP collaboration, M. Tanabashi et al., *Phys. Rev.* **D98** (2018) 030001.
[2] BELLE-II collaboration, W. Altmannshofer et al., 1808.10567.
[3] LHCB collaboration, R. Aaij et al., 1808.08865.
[4] BABAR collaboration, J. Lees et al., *Phys.Rev.Lett.* **109** (2012) 101802 [1205.5442].
[5] BABAR collaboration, J. P. Lees et al., *Phys. Rev.* **D88** (2013) 072012 [1303.0571].
[6] BELLE collaboration, M. Huschle et al., *Phys. Rev.* **D92** (2015) 072014 [1507.03233].
[7] LHCB collaboration, R. Aaij et al., *Phys. Rev. Lett.* **115** (2015) 111803 [1506.08614].
[8] BELLE collaboration, Y. Sato et al., *Phys. Rev.* **D94** (2016) 072007 [1607.07923].
[9] BELLE collaboration, S. Hirose et al., *Phys. Rev. Lett.* **118** (2017) 211801 [1612.00529].
[10] BELLE collaboration, S. Hirose et al., *Phys. Rev.* **D97** (2018) 012004 [1709.00129].
[11] LHCB collaboration, R. Aaij et al., *Phys. Rev. Lett.* **120** (2018) 171802 [1708.08856].
[12] LHCB collaboration, R. Aaij et al., *Phys. Rev.* **D97** (2018) 072013 [1711.02505].
[13] BELLE collaboration, A. Abdesselam et al., 1904.08794.
[14] D. Bigi et al., *Phys. Rev.* **D94** (2016) 094008 [1606.08030].
[15] F. U. Bernlochner et al., *Phys. Rev.* **D95** (2017) 115008 [1703.05330].
[16] D. Bigi et al., *JHEP* **11** (2017) 061 [1707.09509].
[17] S. Jaiswal et al., *JHEP* **12** (2017) 060 [1707.09977].
[18] HFLAV: Heavy Flavor Averaging Group, *Average of $R(D)$ and $R(D^*)$ for spring 2019*, 2019.
[19] CKMFITTER GROUP collaboration, J. Charles et al., *Eur.Phys.J.* **C41** (2005) 1 [hep-ph/0406184].
[20] UTFIT collaboration, M. Bona et al., *JHEP* **0507** (2005) 028 [hep-ph/0501199].
[21] M. Antonelli et al., *Phys.Rept.* **494** (2010) 197 [0907.5386].
[22] FLAVOUR LATTICE AVERAGING GROUP collaboration, S. Aoki et al., 1902.08191.
[23] HPQCD collaboration, E. Dalgic et al., *Phys.Rev.* **D73** (2006) 074502 [hep-lat/0601021].
[24] FERMILAB/MILC collaboration, J. A. Bailey et al., *Phys. Rev.* **D79** (2009) 054507 [0811.3640].
[25] FERMILAB/MILC collaboration, J. A. Bailey et al., *Phys. Rev.* **D92** (2015) 014024 [1503.07839].
[26] RBC/UKQCD collaboration, J. M. Flynn et al., *Phys. Rev.* **D91** (2015) 074510 [1501.05373].
[27] FERMILAB/MILC collaboration, J. A. Bailey et al., *Phys. Rev. Lett.* **109** (2012) 071802 [1206.4992].
[28] MILC collaboration, J. A. Bailey et al., *Phys. Rev.* **D92** (2015) 034506 [1503.07237].
[29] HPQCD collaboration, H. Na et al., *Phys. Rev.* **D92** (2015) 054510 [1505.03925].
[30] C. Bouchard et al., *Phys.Rev.* **D90** (2014) 054506 [1406.2279].
[31] ALPHA collaboration, F. Bahr et al., *Phys. Lett.* **B757** (2016) 473 [1601.04277].
[32] FERMILAB/MILC collaboration, A. Bazavov et al., *Phys. Rev.* **D100** (2019) 034501 [1901.02561].
[33] FERMILAB/MILC collaboration, J. A. Bailey et al., *Phys. Rev.* **D85** (2012) 114502 [1202.6346].
[34] HPQCD collaboration, C. J. Monahan et al., *Phys. Rev.* **D95** (2017) 114506 [1703.09728].
[35] HPQCD collaboration, E. McLean et al., 1906.00701.
[36] S. Hashimoto, *PoS* **LATTICE2018** (2018) 008 [1902.09119].
[37] B. Colquhoun et al., *PoS* **LATTICE2018** (2018) 274 [1811.00227].
[38] ETM collaboration, V. Lubicz et al., *PoS* **LATTICE2018** (2018) 287 [1811.10268].
[39] JLQCD collaboration, T. Kaneko et al., *PoS* **LATTICE2018** (2018) 311 [1811.00794].
[40] JLQCD collaboration, B. Colquhoun et al., 1912.02409.
[41] A. Lytle, "$B \to D^*$ form factors, $R(D^*)$, and $|V_{cb}|$." Plenary Talk Lattice 2019, Wuhan, China, 2019.
[42] A. X. El-Khadra et al., *Phys. Rev.* **D55** (1997) 3933 [hep-lat/9604004].
[43] N. H. Christ et al., *Phys.Rev.* **D76** (2007) 074505 [hep-lat/0608006].
[44] D. B. Kaplan, *Phys. Lett.* **B288** (1992) 342 [hep-lat/9206013].
[45] Y. Shamir, *Nucl. Phys.* **B406** (1993) 90 [hep-lat/9303005].
[46] V. Furman et al., *Nucl. Phys.* **B439** (1995) 54 [hep-lat/9405004].

[47] T. Blum et al., *Phys. Rev.* **D56** (1997) 174 [hep-lat/9611030].
[48] T. Blum et al., *Phys. Rev. Lett.* **79** (1997) 3595 [hep-lat/9706023].
[49] R. C. Brower et al., *Comput. Phys. Commun.* **220** (2017) 1 [1206.5214].
[50] RBC/UKQCD collaboration, C. Allton et al., *Phys. Rev.* **D78** (2008) 114509 [0804.0473].
[51] RBC/UKQCD collaboration, Y. Aoki et al., *Phys.Rev.* **D83** (2011) 074508 [1011.0892].
[52] RBC/UKQCD collaboration, T. Blum et al., *Phys. Rev.* **D93** (2016) 074505 [1411.7017].
[53] RBC/UKQCD collaboration, P. A. Boyle et al., *JHEP* **12** (2017) 008 [1701.02644].
[54] RBC/UKQCD collaboration, N. H. Christ et al., *Phys.Rev.* **D91** (2015) 054502 [1404.4670].
[55] RBC/UKQCD collaboration, J. M. Flynn et al., *Phys. Rev.* **D93** (2016) 014510 [1506.06413].
[56] Y.-G. Cho et al., *JHEP* **05** (2015) 072 [1504.01630].
[57] RBC/UKQCD collaboration, P. Boyle et al., *JHEP* **04** (2016) 037 [1602.04118].
[58] RBC/UKQCD collaboration, Y. Aoki et al., *Phys. Rev.* **D86** (2012) 116003 [1206.2554].
[59] A. X. El-Khadra et al., *Phys.Rev.* **D64** (2001) 014502 [hep-ph/0101023].
[60] D. Bećirević et al., *Phys.Rev.* **D67** (2003) 054010 [hep-lat/0210048].
[61] J. Bijnens et al., *Nucl.Phys.* **B840** (2010) 54 [1006.1197].
[62] C. G. Boyd et al., *Phys.Rev.Lett.* **74** (1995) 4603 [hep-ph/9412324].
[63] C. Bourrely et al., *Phys.Rev.* **D79** (2009) 013008 [0807.2722].
[64] W. A. Bardeen et al., *Phys.Rev.* **D68** (2003) 054024 [hep-ph/0305049].
[65] E. J. Eichten et al., *Phys. Rev.* **D99** (2019) 054025 [1902.09735].
[66] RBC/UKQCD collaboration, J. Flynn et al., *PoS* **LATTICE2015** (2016) 345 [1511.06622].
[67] RBC/UKQCD collaboration, J. Flynn et al., *PoS* **LATTICE2016** (2016) 296 [1612.05112].
[68] RBC/UKQCD collaboration, P. A. Boyle et al., 1812.08791.
[69] P. Boyle et al., 1912.07563.